KSCE Journal of Civil Engineering (2023) 27(12):5319-5328
DOI 10.1007/s12205-023-0316-5

pISSN 1226-7988, eISSN 1976-3808
www.springer.com/12205

Structural Engineering

An Experimental Study on the Deterioration Behaviour of External Tendons Due to Corrosion

Dongwook Kim[a], **Chi-Ho Jeon**[b], **and Chang-Su Shim**[c]

[a]*Member, Civil Smart Engineering Team, Civil Engineering Division, DL E&C Co., Ltd., Seoul 03181, Korea*
[b]*Dept. of Civil and Environmental Engineering, Chung-Ang University, Seoul 06974, Korea*
[c]*Member, Dept. of Civil and Environmental Engineering, Chung-Ang University, Seoul 06974, Korea*

ARTICLE HISTORY

Received 23 February 2023
Accepted 25 August 2023
Published Online 18 October 2023

KEYWORDS

Prestressed concrete bridge
External tendon
Corrosion
Macrocell corrosion
Repair

ABSTRACT

An external tendon failure of the PSC box girder was found due to corrosion in South Korea, and the maintenance authorities promoted a study on evaluation and maintenance methods. One of their concerns was to confirm that the tendons were constantly available through repair when voids or minor corrosion were found in ducts. This study, thus, conducted external tendon experiments with insufficient grout filling and corrosion, and the resulting decrease in deterioration behaviours was investigated. The corrosion was accelerated during the experiment, and the strains and prestressing force were measured. The test results indicated minimal reductions in prestressing force and strain as the corrosion was induced, followed by significant fluctuations when a corroded wire ruptured. Prior to the rupture, the strain development was approximately 130 με. However, after the rupture, the strain increased significantly, reaching a maximum of 4,296 με in compression and 2,776 με in tension. It was also confirmed that enough grout ratio to strands resulted in meaningful stress redistribution among the strands and that the wire rupture caused various strain development due to impact load. Based on the test result, a method for corrosion monitoring after re-grout was also proposed using low-power sensing and strain gauges.

1. Introduction

As the prestressed concrete (PSC) bridges are ageing, research on the corrosion of prestressing tendons is actively conducted. Various corrosion cases of external tendons were introduced in the investigation studies (Reis, 2007; Trejo et al., 2009; Carsana and Bertolini, 2015). Cases presented in these studies have shown that severe corrosion has caused the steel strands to rupture, and no prior action has been taken because it was invisible due to grout and ducts during the inspection. The leading cause of tender corrosion is due mainly to insufficient grout filling and chloride penetration (Menga et al., 2022), and the well-grout-infilled area of the tendon was sufficiently protected from corrosion.

Corrosion-induced rupture of the external tendon of the PSC box girder bridge was found in South Korea, and research was conducted to find the cause (KIBSE, 2020). In the study, the mechanical performance of corroded strands was investigated, and the repairability of the tendons with minor corrosion was examined (Fig. 1). The background of the study is a case in which the void generated in the external tendon was repaired by injecting a high-performance grout, but the steel strand was broken due to the macrocell corrosion phenomenon that causes corrosion at the interface with the existing grout (Trejo et al., 2009). As a result of an experiment to observe macrocell corrosion after repair on the PSC box girder bridge, it was confirmed that macrocell corrosion current flows after the grout is newly injected, and thus corrosion may occur. Three years of observation show that no further progress in corrosion has been made yet, but continuous follow-up is being made because sufficient experimental data has not been obtained. In addition, there is insufficient research on the behaviour changes in the external tendon during the corrosion process, and additional research is required.

In this study, external tendon experiments with insufficient grout filling and corrosion were planned, and the resulting decrease in deterioration behaviours was investigated. The corrosion was

CORRESPONDENCE Chi-Ho Jeon chihobeer@cau.ac.kr Dept. of Civil and Environmental Engineering, Chung-Ang University, Seoul 06974, Korea

(a) (b)

Fig. 1. Field Experiments on Corrosion Tendon Repair (KIBSE, 2020): (a) Long-term Observation without Grout, (b) Long-term Observation with Grout Reinjection

accelerated during the experiment, and the strains and prestressing force were measured. A method for corrosion monitoring after re-grout was also proposed by analysing the data obtained through the experiment.

2. Literature Review

2.1 Mechanical Properties of Corroded Strands

Previous studies have been conducted on the mechanical behaviours of corroded prestressing steel strands (Jeon et al., 2019, 2020, 2023). These studies conducted finite element analysis and tensile tests on corroded strand specimens recovered from the same bridges as KIBSE (2020), and it showed the relationship between tensile strength, elongation, and cross-sectional loss. Existing experiments on corrosion rebars (Zhang et al., 2012) show a clear negative linear correlation between corrosion extent and mechanical properties (survival strength, elongation, and extreme strength). On the other hand, the strands had a different aspect. Since a steel strand comprises seven steel wires, the corrosion extent may vary for each steel wire, and the most corroded steel wire is ruptured first. When defining the moment of steel wire fracture as the ultimate strength, the decrease in extreme strength and elongation was proportional to the corrosion extent of the steel wire. Especially, the elongation decreased rapidly rather than the strength; The elongation may reduce by more than 50% if the wire-unit section loss reaches 4%. (Jeon et al., 2020). In addition, the decrease in yield strength did not show a clear proportionality to the corrosion level because of stress redistribution between steel wires. These results were similar to other studies regarding the mechanical properties of corroded strands (Wang et al., 2020; Franceschini et al., 2022).

2.2 Effect of Tendon Corrosion in PSC Beams

Recently, designating and managing key performance indicators was proposed to increase the maintenance efficiency of bridges (Limongelli and Orcesi, 2017; Strauss et al., 2017). In the case of PSC bridges, the prestressing tendon is a governing element in the structural behaviour (Rakoczy and Nowak, 2013) and the cases of sudden collapse due to tendon corrosion (Cederquist, 2000; Colajanni et al., 2016; Rymsza, 2020) have been reported around the world. Therefore, changes during the corrosion process must be studied to use tendons as a key performance indicator.

Several experiments on aged PSC girders (Poston and West, 2005; Pape and Melcher, 2013; Jeon et al., 2021) and small-scale lab tests (Minh et al., 2007; Coronelli et al., 2009; Wang et al., 2014; Moawad et al., 2018) were conducted to study the effect of tendon damages on behaviour changes of PSC members. The studies showed a decrease in the load-carrying capacity, early crack generation, a decrease in ductile behaviour, and changes in failure mode from ductile to brittle depending on the extent of corrosion. However, all of these studies are about tests with internal tendons, and the effect on the entire structure was insignificant if the corrosion was located in a place with less bending moment. These studies also have a commonality that deals with post-corrosion behaviour.

The external tendon with a relatively low confinement effect by concrete may have different results from the above. The loading tests on PSC box girders with corroded external tendons are challenging due to their magnitude, and studies have been conducted to examine them indirectly through specimens depicting external tendons. Li et al. (2022) conducted a corrosion test on a single strand without the grout, and the result showed gradual prestressing force reduction according to the induction time. (Lee and Kang, 2019) observed corrosion-induced changes in vibration characteristics on external tendon specimens containing several steel strands, and the prestressing force observed in this process also decreased according to the corrosion level. These characteristics indicate that even corrosion at a cross-section with less flexural moment can affect the structural behaviour, unlike the internal tendon.

However, these studies did not consider grout filling sufficiently; therefore, a high correlation between corrosion level and tension was observed, similar to the unbonded tendon behaviour. Considering the literature on the relationship between corrosion and the bond strength of steel strands (Li and Yuan, 2013; Wang et al., 2017a, 2017b; Yi et al., 2020), the degradation of external tendons can be considered as between bonded and unbonded tendon behaviours, and research on this is still insufficient.

In this paper, therefore, a small-scale experimental program was designed, including three external tendon specimens with sufficient grout filling. After the grout curing, the corrosion of

the strands was artificially induced, and strain developments and tension were measured to examine the corrosion behaviour of bonded tendons.

3. Experimental Program

A reaction frame with three tendons (T1, T2, and T3) was manufactured to simultaneously observe corrosion and non-corrosion behaviours, as shown in Fig. 2. The reaction frame was designed to have small deformation enough to avoid the prestressing load change of a tendon affecting one other. The three H beams holding each tendon had a dimension of 300 × 300 × 10 × 15 mm (height × flange width × web thickness × flange thickness), and 30 mm thickness of steel plates were welded at both anchor and tension ends. Each steel plate had a hole, so the tendons penetrated. Four H beams, with dimensions of 200 × 200 × 8 × 2 mm, were assembled for the diaphragm at both ends and midspan. Sections A, B, and C are regarding the locations of corrosion induction

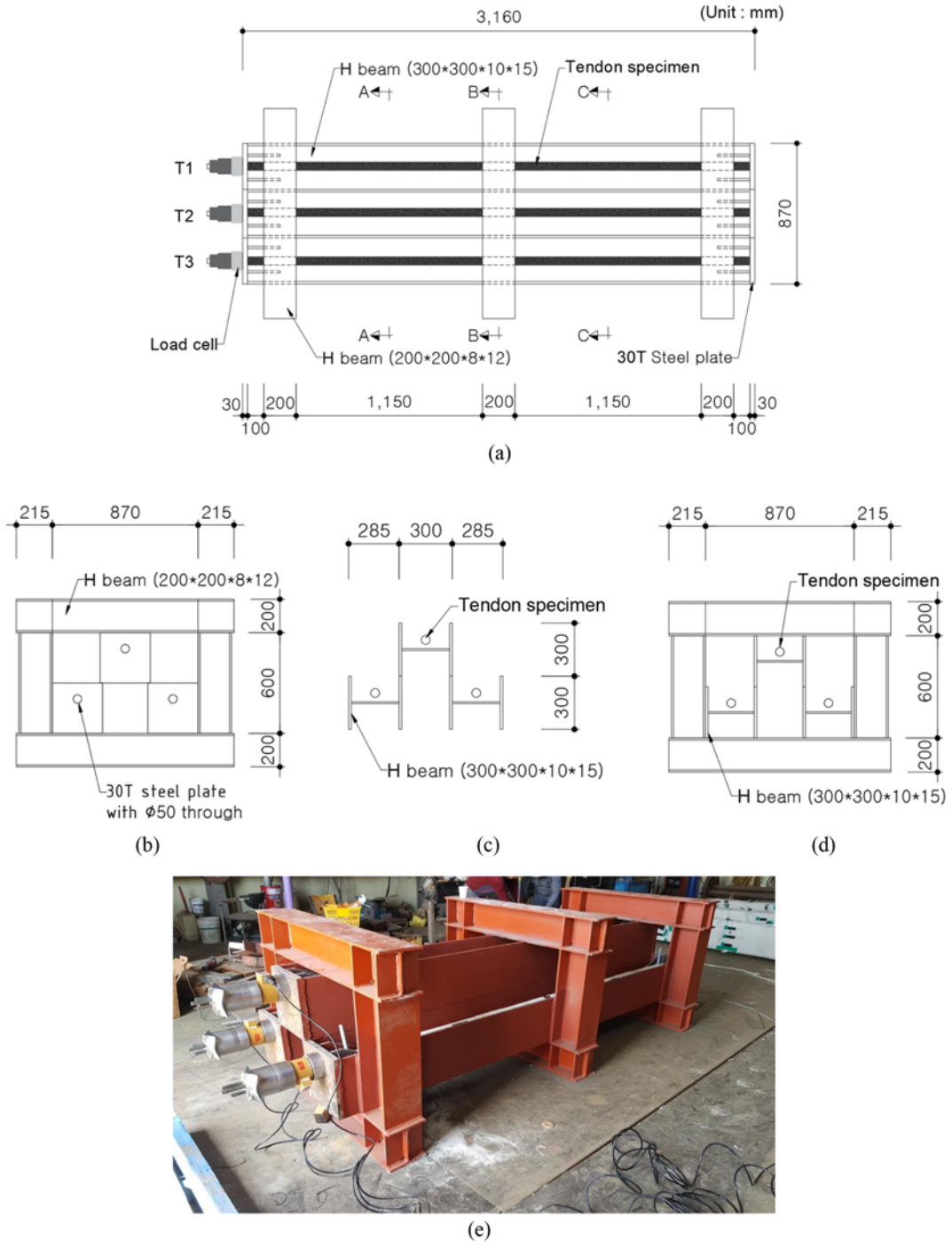

Fig. 2. Reaction Frame for the Test: (a) Plan View, (b) Front View, (c) Sections A & C, (d) Section B, (e) Manufactured Reaction Frame

and gauge deployments. A, B, and C were located 1/4, 1/2, and 3/4 of the total tendon length from the anchor end, respectively, and the tendon length was 3,160 mm. Table 1 shows the specimen details in the experimental program. Each tendon has three prestressing steel strands, and the average measured mechanical properties based on tensile tests are listed in Table 2. The initial prestressing forces were 434.14, 428.99, and 432.43 kN, applied to T1, T2, and T3, respectively, thereby causing the initial stresses of 1,004.36, 1,030.98, and 1,039.25 MPa, respectively. T1 is a reference specimen without corrosion. T2 and T3 had artificially induced corrosion at sections C and B, respectively. Load cells were placed at each anchor end to measure prestressing force reduction. Polyvinyl chloride pipes with an internal diameter of 50 mm were used as ducts for each tendon.

Table 1. Specimen Details

Specimens	# of strands	Location of corrosion	# of corrosion acceleration strands	Initial prestressing force
T1	3	None	None	434.14 kN
T2	3	Section C (3/4 span)	2	428.99 kN
T3	3	Section B (1/2 span)	1	432.43 kN

Table 2. Average Measured Mechanical Properties of the Non-corroded Strand Specimens

Diameter (mm)	Nominal Sectional Area (mm^2)	0.2% Proof Stress (MPa)	Strain Corresponding to 0.2% Proof Stress	Ultimate Strength (MPa)	Ultimate Strain
15.2	138.7	1,726	0.0099	1,865	0.075

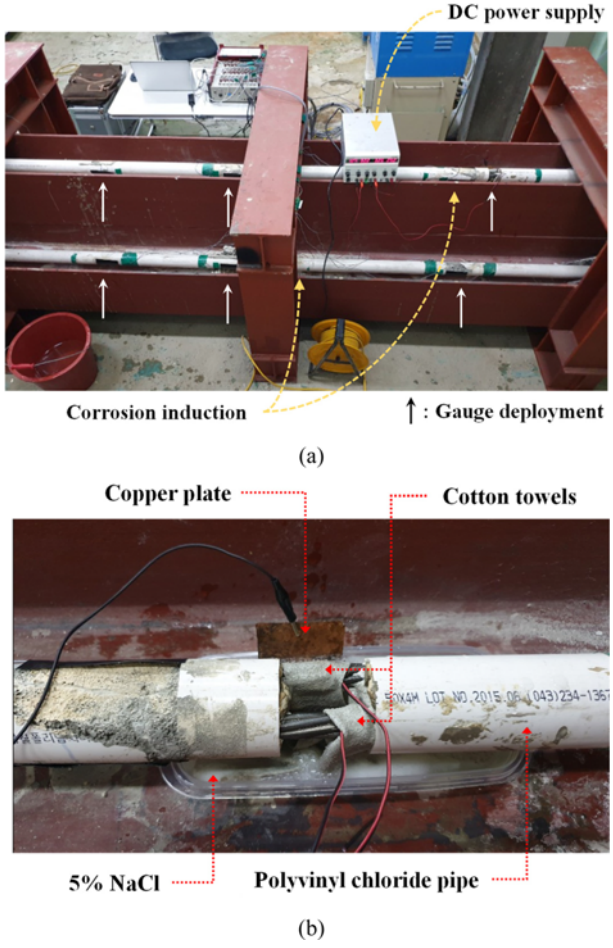

Fig. 3. Test Setup: (a) Gauge Deployments, (b) Corrosion Acceleration of Strands

Figure 3 shows the detailed tendon specimens, gauge deployments, and corrosion acceleration test setup. Each tendon had two strain gauges at both the right and left side surfaces at each section, resulting in eighteen gauges, as shown in Fig. 3(a). The gauges were attached after the grout had cured and the polyvinyl chloride pipe had been removed. The temperature variation was also measured to eliminate its effect on the behaviour of the specimens. The grout was not filled at the corrosion acceleration locations to expose the strands to the air, and the corrosion test setup was prepared, as shown in Fig. 3(b). A copper plate was immersed in 5% NaCl solution and connected to the negative electrode of the direct current power supply, and the strand was connected to the positive electrode. The cotton towel was hung on the strands, and its tip was also immersed in the 5% NaCl solution, which induced localised corrosion. The corrosion had been accelerated at two strands in T2 simultaneously and one in T3 and continued until a strand was ruptured. The strain and prestressing force were measured every 5 minutes during the corrosion test.

4. Test Result

Figure 4 shows prestressing force change during the corrosion acceleration test from the load cells, and the pictures on the right were taken before and after the test. As expected, T1 had no reduction of prestressing force during the test, while other corroded specimens resulted otherwise. T2 and T3 showed two prestressing force drops when the corroded wires ruptured after a certain period of plateau. However, the amount of force drops was different; prestressing forces of T2 and T3 were reduced by 14% and 24%, respectively. As depicted in Fig. 3, T2 had the two cotton towels hanging on the strands to simultaneously accelerate corrosion, resulting in more severe corrosion than T3.

Interestingly, the strand without the cotton towel below corroded faster than the two strands intended to induce the current flow. The reason was that the cotton towels touched the lower strand, which caused a corrosion reaction earlier than the other strands because the distance between the NaCl solution and the lower strand was closer. Therefore, two times the current flow was induced to the strands (because two towels touched), and the steel wire rupture occurred earlier than T3. This phenomenon also occurred at T3; the lower strand was corroded earlier than intended.

Figure 5 shows strain developments of the grout surfaces during the test. Temperature effects were eliminated using data

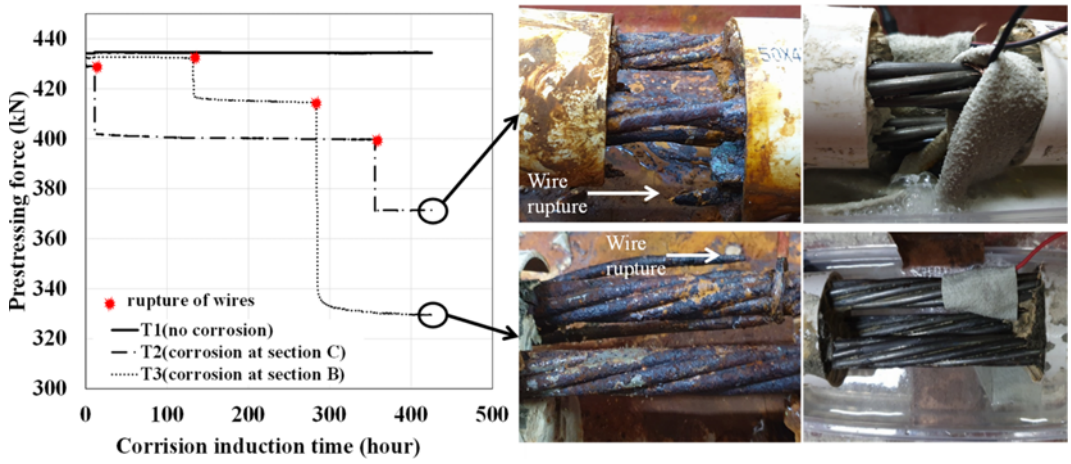

Fig. 4. Prestressing Force Change and Pictures of Specimens during the Corrosion Test

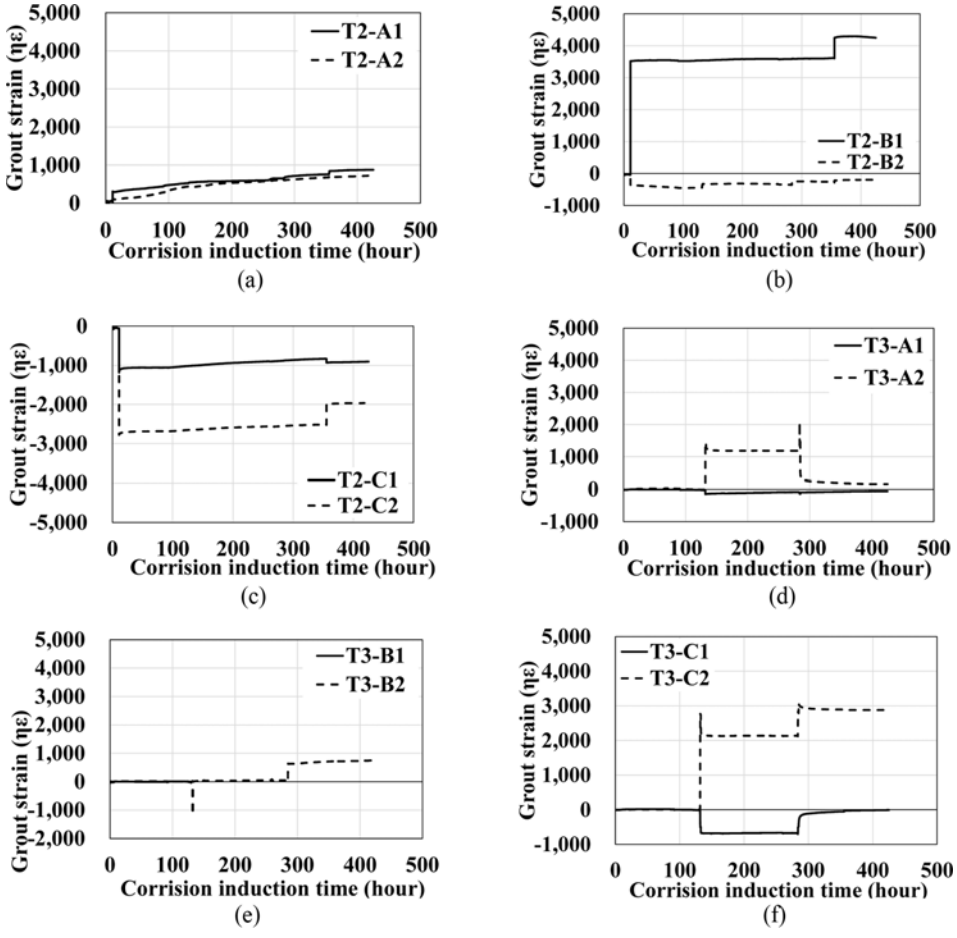

Fig. 5. Strain Developments during the Corrosion Test: (a) Section A in T2, (b) Section B in T2, (c) Section C in T2, (d) Section A in T3, (e) Section B in T3, (f) Section C in T3

from thermometers and strain gauges attached to plain concrete cylinders. Before the first wire rupture, strain development rarely occurred; the highest strain was about 130 με. After that, however, the strain increased at most 4,296 and 2,776 με in compression and tension, respectively, and the change also occurred regarding the subsequent wire rupture. The detailed meaning of strain development was discussed in section 4.

5. Discussion

5.1 Stress Redistribution

A related study (Li et al., 2022) conducted a corrosion test on a

single strand without the grout, and the result showed gradual prestressing force reduction according to the induction time, even though there was no rupture during the test. This result is evident because the increasing strain due to cross-sectional loss is transferred to the anchor wedge designed only to withstand inner-ward loads. In other words, the anchor system caused the corrosion-induced strain to dissipate during the test. The same aspect was found in the experiment specimen with multiple strands (Lee and Kang, 2019). However, the results of this experiment rarely considered the influence of grout. The prestressing force did not change during the corrosion test in this study before rupture. It means the plateau of Fig. 4 indicates stress redistribution occurred between the strands due to the grout.

The grout has a role in stress redistribution. Fig. 6 shows the static force equilibrium condition of the tested tendon in this study. Because the grout was poured after the initial prestressing force was applied, the initial stress in the grout was zero. However, once the corrosion is induced, the cross-sectional loss (ΔA_s) causes prestressing loss of the strand, producing a compressive load on the grout. This compressive load leads to the deformation of the grout and the strands simultaneously, so the tension of the strands and compression of the grout carries the compressive load. Eq. (1) shows the numerical expression of the static equilibrium condition. The corrosion-induced strain ($\Delta\varepsilon$) is derived from Eq. (1) as shown in Eq. (2). Since the rest of the strands carry as much as the reduced prestress from the corroded strand, the total initial prestressing force does not change during the corrosion induction, even if Δε occurs.

$$E_s \cdot \varepsilon \cdot \Delta A_s = E_s \cdot \Delta\varepsilon \cdot (n-1)A_s + E_c \cdot \Delta\varepsilon \cdot A_{net,grout} \quad (1)$$

$$\Delta\varepsilon = \frac{\rho_s \cdot \alpha \cdot A_s}{\rho_s \cdot (n-1)A_s + A_{net,grout}}\varepsilon \quad (2)$$

Where,

$A_{net,grout}$ = A net grout cross-sectional area (the tendon area subtracted by the total strands area)
E_c = Elastic modulus of the grout
E_s = Elastic modulus of strands
n = The number of strands in the tendon

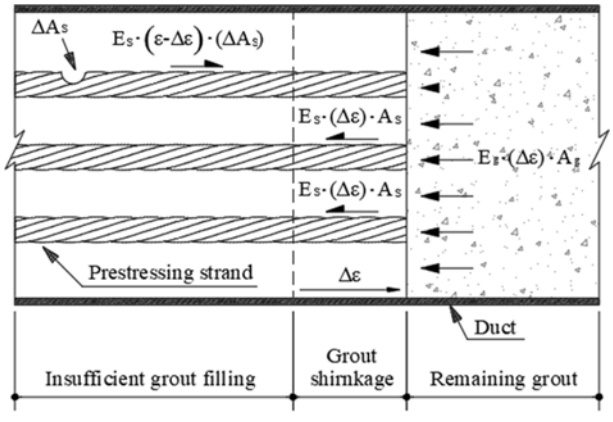

Fig. 6. Equilibrium Condition of a Tendon with Cross-sectional Loss due to Corrosion

α = The coefficient for the extent of the corrosion, $\alpha \geq 0$
ΔA_s = A cross-sectional loss due to corrosion
ε = Initial strain due to prestressing force
$\Delta\varepsilon$ = The compressive strain increment of the grout due to corrosion
ρ_s = Material stiffness ratio (E_s/E_g)

As explained in section 3, $\Delta\varepsilon$ before the first wire rupture was about 130 με at the highest. According to previous studies on the tensile behaviour of corroded strands (Jeon et al., 2019, 2020, 2023), the elongation capacity decreases rapidly from 5% of the cross-sectional loss. Because it was difficult to measure the cross-sectional loss during the test, if α in Eq. (2) is assumed to be 5%, $\Delta\varepsilon$ is calculated as 120 με, which is similar to the test result. The number of strands considered in this study was 3, but the practically used number of strands and the dimension of tendons are much larger than this, which leads to $\Delta\varepsilon$ negligible in Eq. (2). Therefore, it may not indicate that non-destructive evaluation for corrosion detection is applicable if the evaluation considers structural or mechanical behaviour changes before wire rupture.

This equilibrium condition only lasts before the rupture. During the corrosion induction, stress redistribution also occurs between the steel wires that make up the strand. The stress of corroded steel wires increases as the cross-sectional loss progresses, and when the stress reaches the ultimate strength, a rupture occurs. At that moment, a wire rupture causes an impact load on the grout, which is no longer in a static state. Therefore, Eqs. (1) and (2) are invalid, and the impact load results in slip, crack in the grout and prestressing loss.

5.2 Interaction between the Grout and Strands

Stress redistribution in Fig. 6 is valid only if the bond strength is enough. Some literature conducted studies on bond strength degradation regarding corrosion (Wang et al., 2017a, 2017b; Dai et al., 2019; Yi et al., 2020). According to the studies, the bond strength degradation is related to the effects of corrosion-induced cracking due to volume expansion and rotation mechanism of the helical-shaped strand. The studies also found that the tensile force of the corroded strand transmitted through two zones, the slipping zone and the effective bond zone, and proposed numerical prediction models of the bond strength for a single strand. Because the specimens in this paper had three strands in a tendon, it is challenging to adopt the proposed model as it is, and no other studies have been conducted on multiple strands. However, their idea and concept can be applied to outline the overall behaviour. Fig. 7 shows four phases of corrosion-induced bond strength degradation, and the details of each phase are as follows.

1. Initiation of corrosion (Fig. 7(a)): This state indicates the same as Fig. 6. Where 'T' and 'C' are tension and compression, and ΔF_{pe} is a compressive force on the grout due to the corrosion-induced reduction of effective prestressing force. F_{eb} is the reaction force against ΔF_{pe} generated with the contribution of effective bond strength. According to

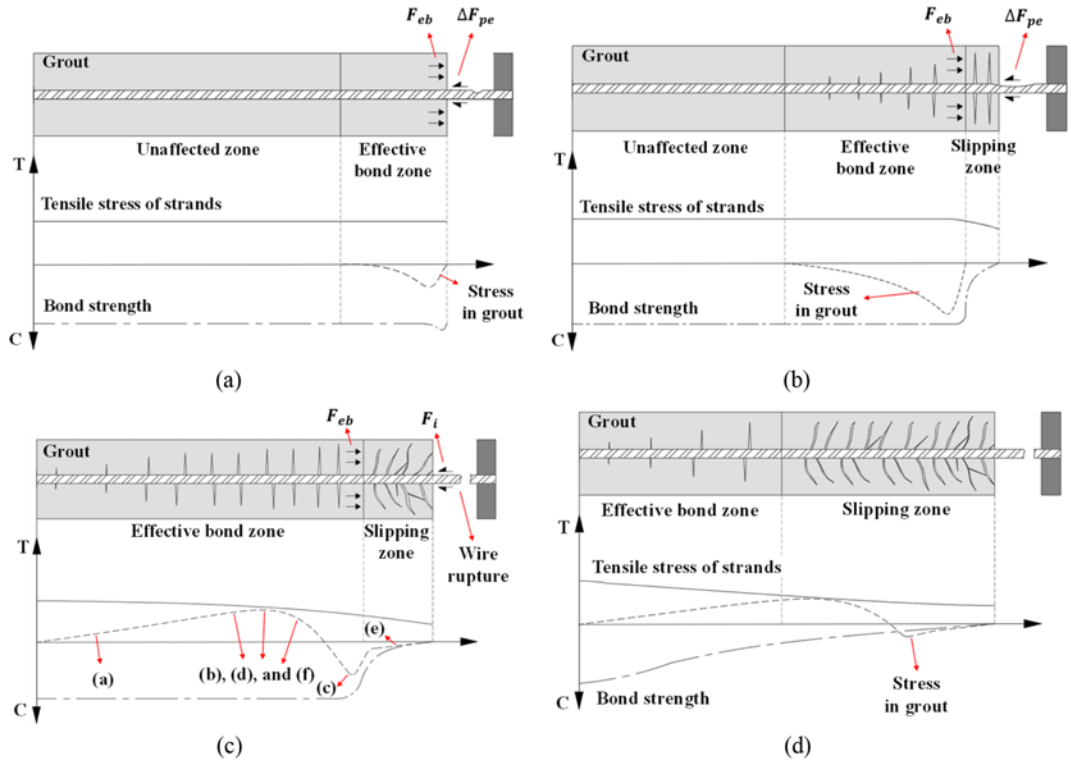

Fig. 7. Four Phases of Corrosion-induced Bond Strength Degradation: (a) Initiation of Corrosion, (b) Development of Slip Behaviour, (c) Moment of Wire Rupture, (d) Stabilisation after Wire Rupture

Dai et al. (2019), the effective bond strength of surrounding grout increases up to 1.4 times because of volume expansion at an early stage of corrosion and decreases after 7.3% of corrosion-induced loss measured based on mass loss. In the case of cross-section-based corrosion loss, Yi et al. (2020) showed the ultimate bond strength decreased if the corrosion loss was higher than 2% (without stirrup), which was based on a numerical prediction model for the ideal corrosion environment of a single strand. These findings support that grout can play a sufficient role in stress redistribution between strands in the initial state of corrosion. In this phase, there is no slip, the stress in the grout increases in compression, and the average tensile stress of strands is constant due to stress redistribution.

2. Development of slip (Fig. 7(b)): Once the effective bond strength degradation exceeds the threshold, corrosion-induced cracking occurs, forming a slipping zone. According to Wang et al. (2017a, 2017b), the adhesion action between grout and strands will vanish after the slip, and twisting of strands occurs. Therefore, local crushing and microcracking occur, and the bond strength continues to decrease until only providing longitudinal friction force, which is very small. Considering global behaviour, however, this is not considerable. This behaviour is related to the plateau before the wire rupture in Fig. 6, showing around 0.3% of prestressing force reduction before the first wire rupture. In the case of local behaviour, the strains rarely developed (less than 30 με) at all deployed locations before the wire rupture, which seems to indicate that the grout ratio to the strands was relatively high when considering Fig. 6.
3. Moment of wire rupture (Fig. 7c): If the tensile stress at the corroded section reaches the ultimate stress of the strand due to the section loss, the wire ruptures, and then suddenly released ΔF_{pe} acts as an impact load, F_i, to the remaining grout. The impact load caused dynamic behaviour, resulting in action and reaction within the grout. Literature (Lu and Xu, 2004) found that the strain rate effect due to the impact load made the tensile strength of concrete increase about seven times at a strain rate of 100 s^{-1}. Thus, the strains that showed more than 3,000 με in Fig. 5 are not considered errors. The differences in strain values between gauges at the same position seem to be caused by the asymmetry of the strand positions.

The symbols from (a) to (f) indicate Figs. 5(a) to 5(f) and show the stress status considering the distance of the gauges from the location of the wire rupture. (e) was located at section B of T3, which was in the slipping zone and showed no stress development. (c) was at section C of T2 and showed compressive strain due to the reaction force in the effective bond zone. (b), (d) and (f) were located longer than (e) and (c) from the wire rupture and showed high tensile strains. The farthest distance from the wire rupture was (a), located at section A in T2, showing relatively minor strain development. Those stress developments seem to mean that the effective bond zone was

formed to the end; thereby, the prestressing force decreased simultaneously as the steel wire ruptured.

4. Stabilisation (Fig. 7(d)): After the wire rupture, cracking and bond behaviours are stabilised, and the slipping zone forms wider. After the first wire rupture, the force reduction rate increased due to the widened slipping zone, and its amount was 1%. However, this increase is meaningless from a structural engineering point of view because the serviceability of the tendon was already ended when the wire ruptured.

5.3 Corrosion Monitoring for Repaired Grout

As mentioned earlier, repair through re-grout for the regions where voids or minor corroded strands are present requires structural health monitoring in consideration of macrocell corrosion. The previous study (KIBSE, 2020) proposed a method to detect corrosion initiation by measuring the current flow generated in the steel wire in the repaired region. This method enables preemptive response by early detection of corrosion occurrence but requires the proficiency of the operators and additional equipment for measurement. Therefore, considering the long-term service life of the bridge, it is reasonable to consider a more straightforward and durable monitoring method together.

Based on the experimental results, this study proposes a long-term monitoring method utilising strain gauges, as shown in Fig. 8. In this method, the duct is opened, and a concrete gauge is installed on the surface of the existing grout before the repair grout is injected. The concrete gauges are deployed at a certain distance from the interface between the existing grout and the repair grout, where macrocell corrosion is likely to occur, to avoid areas where the grout does not have strain variation due to reduced bond strength. The strain gauges traditionally have been measured using data loggers, which also need electric power and equipment. Recently, ultra-low-power sensing technology acquiring measurement data using QR code and network technology has been studied (Khan et al., 2021; Won et al., 2021). This technology collects and records data at specific cycles and can be maintained for a long time at low power. In addition, there is no additional work performed by workers other than equipment attached to the site, so it is beneficial for the maintenance of bridges. Since the corrosion does not occur in a short period, it is possible to check the progress of the corrosion with a low measurement cycle (e.g., once a month). Therefore, using ultra-low-power sensing technology, long-term monitoring is possible with low cost and human resources. Monitoring using strain gauges has the following advantages. 1) Regardless of the operator's proficiency, it is possible to intuitively check whether corrosion occurs by checking the trend of strain; 2) The work is relatively simple because only concrete gauges need to be attached after the repair is completed. 3) It is possible to apply to areas where direct observation is difficult such as the diaphragm and the deviation block. On the other hand, if the ratio of grout in the cross-section is high and the effect of stress

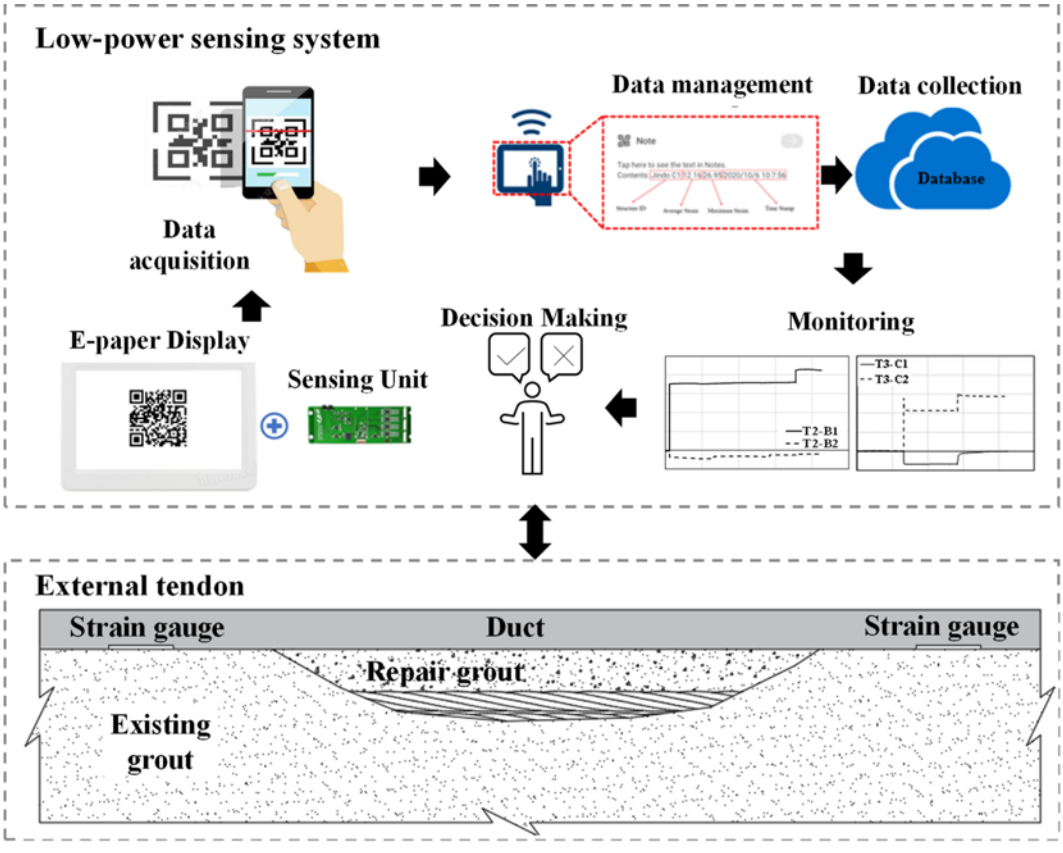

Fig. 8. Schematic of Repaired Tendon Monitoring Using Strain Gauges

redistribution is significant, the strain may not change in the early stages of corrosion; detection may be possible after wire rupture occurs. Further research is required on the grout ratio in which the strain rate may change due to corrosion on the grout

6. Conclusions

This study planned an experiment to investigate the deterioration behaviour of prestressing tendons in corrosion progress. The experimental program includes three tendon specimens manufacturing and corrosion acceleration procedures on two of them. During the corrosion induction, the strain and prestressing force were measured from deployed gauges on the grout surface, and the load cell at anchor ends. The primary research findings are as follows.

1. The prestressing force rarely reduced during the corrosion acceleration but suddenly dropped when corrosion-induced wire rupture occurred, which was a significant difference from the literature. The reason was the presence of enough grout in the specimens resulted in stress redistribution between strands, whereas the literature showed a lack of grout. Eqs. (1) and (2) showed numerical expressions of stress redistribution based on the equilibrium condition.
2. The strain developments were analysed from the deployed concrete gauges on the surface of the grout. When corrosion occurred, the reduced tension due to the cross-sectional loss was transmitted through the slipping and effective bond zones. Before the wire rupture, the strains rarely developed at all gauge locations because the grout ratio to strands was high. However, the wire rupture changed the tendon from static to impact load condition, resulting in various strain developments. Because the bond strength was reduced at the slipping zone, the strain development was lower than in other locations. On the other hand, the strain was highly developed in the effective bond zone, and its increment was gradually reduced with the distance from the corrosion.
3. Based on the test result, a monitoring method for repaired external tendons was proposed. Considering the macrocell corrosion, the strain gauges are deployed on the surface of the existing grout at a certain distance from the interface with the re-grout. For a long-term monitoring system, it was suggested to utilise ultra-low-power sensing technology, enabling low cost and human resources with a low measurement cycle and effective data acquisition.

Acknowledgments

This research was supported by Basic Science Research Program through the National Research Foundation of Korea (NRF) funded by the Ministry of Education (2022R1A6A3A03060360).

ORCID

Dongwook Kim https://orcid.org/0000-0002-0721-5114
Chi-Ho Jeon https://orcid.org/0000-0002-2191-0367
Chang-Su Shim https://orcid.org/0000-0001-7557-9553

References

Carsan M, Bertolini L (2015) Corrosion failure of post-tensioning tendons in alkaline and chloride-free segregated grout: A case study. *Structure and Infrastructure Engineering* 11(3):402-411, DOI: 10.1080/15732479.2014.887736

Cederquist SC (2000) Motor speedway bridge collapse caused by corrosion. *Materials Performance* 36(7):18-19

Colajanni P, Recupero A, Ricciardi G, Spinella N (2016) Failure by corrosion in PC bridges: A case history of a viaduct in Italy. *International Journal of Structural Integrity* 7(2), DOI: 10.1108/IJSI-09-2014-0046

Coronelli D, Castel A, Vu NA, François R (2009) Corroded post-tensioned beams with bonded tendons and wire failure. *Engineering Structures* 31(8):1687-1697, DOI: 10.1016/j.engstruct.2009.02.043

Dai L, Wang L, Bian H, Zhang J, Zhang X, Ma Y (2019) Flexural Capacity prediction of corroded prestressed concrete beams incorporating bond degradation. *Journal of Aerospace Engineering* 32(4):4019027, DOI: 10.1061/(asce)as.1943-5525.0001022

Franceschini L, Vecchi F, Tondolo F, Belletti B, Sánchez Montero J (2022) Mechanical behaviour of corroded strands under chloride attack: A new constitutive law. *Construction and Building Materials* 316, DOI: 10.1016/j.conbuildmat.2021.125872

Jeon C-H, Lee J-B, Lon S, Shim C-S (2019) Equivalent material model of corroded prestressing steel strand. *Journal of Materials Research and Technology*, 8(2). DOI: 10.1016/j.jmrt.2019.02.010

Jeon C-H, Nguyen CD, Shim CS (2020) Assessment of mechanical properties of corroded prestressing strands. *Applied Sciences (Switzerland)* 10(12), DOI: 10.3390/APP10124055

Jeon CH, Oeurn S, Shim CS (2023) Test database for corroded prestressing steel strands recovered from aged bridges. *Journal of Materials in Civil Engineering* 35(2):05022003, DOI: 10.1061/(ASCE)MT.1943-5533.0004557

Jeon CH, Sim C, Shim C-S (2021) The effect of wire rupture on flexural behavior of 45-year-old post-tensioned concrete bridge girders. *Engineering Structures*, 245, DOI: 10.1016/j.engstruct.2021.112842

Khan S, Won J, Shin J, Park J, Park JW, Kim SE, Jang Y, Kim DJ (2021) Ssvm: An ultra-low-power strain sensing and visualization module for long-term structural health monitoring. *Sensors* 21(6):1-16, DOI: 10.3390/s21062211

Korean Institute of Bridge and Structural Engineers (KIBSE) (2020) *Detailed Investigation and Monitoring of External Tendons on PSC Box Girder Bridges of Internal Ring Road*, https://www.sisul.or.kr/open_content/main/bbs/bbsMsgDetail.do?msg_seq=6&bcd=presentcon

Lee JK, Kang JW (2019) Experimental evaluation of vibration response of external post-tensioned tendons with corrosion. *KSCE Journal of Civil Engineering*, DOI: 10.1007/s12205-019-0735-5

Li F, Yuan Y (2013) Effects of corrosion on bond behavior between steel strand and concrete. *Construction and Building Materials* 38:413-422, DOI: 10.1016/j.conbuildmat.2012.08.008

Li J, Miki T, Yang Q, Mao M (2022) Experimental study on prestressing force of corroded prestressed concrete steel strands. *Journal of Advanced Concrete Technology* 20(9):550-563, DOI: 10.3151/jact.20.550

Limongelli MP, Orcesi A (2017) A proposal for classification of key performance indicators for road bridges. *39th IABSE Symposium - Engineering the Future* 328-335, DOI: 10.2749/vancouver.2017.0328

Lu Y, Xu K (2004) Modelling of dynamic behaviour of concrete materials under blast loading. *International Journal of Solids and Structures* 41(1):131-143, DOI: 10.1016/j.ijsolstr.2003.09.019

Menga A, Kanstad T, Cantero D, Bathen L, Hornbostel K, Klausen A (2022) Corrosion-induced damages and failures of posttensioned bridges: A literature review. *Structural Concrete*, DOI: 10.1002/suco.202200297

Minh H, Mutsuyoshi H, Niitani K (2007) Influence of grouting condition on crack and load-carrying capacity of post-tensioned concrete beam due to chloride-induced corrosion. *Construction and Building Materials* 21(7):1568-1575, DOI: 10.1016/j.conbuildmat.2005.10.004

Moawad M, El-Karmoty H, el Zanaty A (2018) Behavior of corroded bonded fully prestressed and conventional concrete beams. *HBRC Journal* 14(2):137-149, DOI: 10.1016/j.hbrcj.2016.02.002

Pape TM, Melcher RE (2013) Performance of 45-year-old corroded prestressed concrete beams. *Proceedings of the Institution of Civil Engineers: Structures and Buildings* 166(10):547-559, DOI: 10.1680/stbu. 11.00016

Poston RW, West JS (2005) Investigation of the charlotte motor speedway bridge collapse. In *Structures Congress 2005: Metropolis and Beyond*, DOI: 10.1061/40753(171)243

Rakoczy AM, Nowak AS (2013).Reliability-based sensitivity analysis for prestressed concrete girder bridges. *PCI Journal* 58(4):81-92, DOI: 10.15554/pcij.09012013.81.92

Reis RA (2007) Corrosion Evaluation and Tensile Results of Selected Post-Tensioning Strands at the SFOBB Skyway Seismic Replacement Project Phase I11 Report

Rymsza J (2020) Causes of the morandi viaduct disaster in genoa as a contribution to the design of pre-stressed structures. *Roads and Bridges - Drogi i Mosty* 19(1):5-25, DOI: 10.7409//rabdim.020.001

Strauss A, Mandić Ivanković A, Matos JC, Casas JR (2017, March) Performance indicators for road bridges - overview of findings and future progress. JOINT COST TU1402 COST TU1406 IABSE WC1 WORKSHOP: The Value of Structural Health Monitoring for the Reliable Bridge Management, DOI: 10.5592/co/bshm2017.3.1

Trejo D, Beth Hueste MD, Gardoni P, Pillai RG, Reinschmidt K, Been Im S, Kataria S, Hurlebaus S, Gamble M, Tat Ngo T (2009) Effect of Voids in Grouted, Post-Tensioned Concrete Bridge Construction: Volume 2 - Inspection, Repair, Materials, and Risks, https://rosap.ntl.bts.gov/view/dot/16988

Wang L, Li T, Dai L, Chen W, Huang K (2020) Corrosion morphology and mechanical behavior of corroded prestressing strands. *Journal of Advanced Concrete Technology* 18(10):545-557, DOI: 10.3151/jact.18.545

Wang L, Zhang X, Zhang J, Dai L, Liu Y (2017a) Failure analysis of corroded PC beams under flexural load considering bond degradation. *Engineering Failure Analysis* 73:11-24, DOI: 10.1016/j.engfailanal.2016.12.004

Wang L, Zhang X, Zhang J, Ma Y, Xiang Y, Liu Y (2014) Effect of insufficient grouting and strand corrosion on flexural behavior of PC beams. *Construction and Building Materials* 53:213-224, DOI: 10.1016/j.conbuildmat.2013.11.069

Wang L, Zhang X, Zhang J, Yi J, Liu Y (2017b) Simplified model for corrosion-induced bond degradation between steel strand and concrete. *Journal of Materials in Civil Engineering* 29(4), DOI: 10.1061/(asce)mt.1943-5533.0001784

Won J, Park JW, Park J, Shin J, Park M (2021) Development of a reference-free indirect bridge displacement sensing system. *Sensors* 21(16), DOI: 10.3390/s21165647

Yi J, Wang L, Floyd RW (2020) Bond strength model of strand in corrosion-induced cracking concrete. *ACI Structural Journal* 117(6):119-132, DOI: 10.14359/51728060

Zhang W, Song X, Gu X, Li S (2012) Tensile and fatigue behavior of corroded rebars. *Construction and Building Materials* 34:409-417, DOI: 10.1016/j.conbuildmat.2012.02.071